

# Dynamics of formation and decay of coherence in a polariton condensate

E. del Valle,<sup>1</sup> D. Sanvitto,<sup>2</sup> A. Amo,<sup>3</sup> F.P. Laussy,<sup>1</sup> R. André,<sup>4</sup> C. Tejedor,<sup>5</sup> and L. Viña<sup>2</sup>

<sup>1</sup>*School of Physics and Astronomy, University of Southampton, SO171BJ, Southampton, UK.*

<sup>2</sup>*Dep. Física de Materiales, Universidad Autónoma de Madrid, 28049, Madrid, Spain.*

<sup>3</sup>*Laboratoire Kastler Brossel, Université Pierre et Marie Curie,*

*Ecole Normale Supérieure et CNRS, UPMC Case 74, 75252 Paris Cedex 05, France.*

<sup>4</sup>*CEA-CNRS. Institut NEEL-CNRS, BP166. 38042 Grenoble Cedex 9, France.*

<sup>5</sup>*Dep. Física Teórica de la Materia Condensada,  
Universidad Autónoma de Madrid, 28049, Madrid, Spain*

(Dated: November 12, 2018)

We study the dynamics of formation and decay of a condensate of microcavity polaritons. We investigate the relationship between the number of particles, the emission linewidth and its degree of linear polarization which serves as the order parameter. Tracking the condensate formation, we show that coherence is not determined only by occupation of the ground state, bringing new insights into the determining factors for Bose-Einstein condensation.

Whereas a lot is known of the thermodynamics of quantum fluids—at equilibrium and in infinite size systems—the dynamics of formation of a Bose-Einstein condensate (BEC) is still vastly an open question. This dynamics is not easily detectable in atomic BEC and has not been studied experimentally, due to the very short timescale in which cold atomic gases reach thermal equilibrium. A good alternative to investigate the process of condensate formation is that of microcavity-polaritons [1], although this system differs from atomic condensates due to its intrinsically out-of-equilibrium character. Polaritons arise from the strong coupling of photons and electrons in semiconductor microcavities [2] and have recently shown to undergo a non-equilibrium phase transition with a spontaneous buildup of coherence in the ground state [3, 4, 5, 6, 7], similar to what has been observed in atomic BEC [8, 9]. Thanks to the small polariton lifetime, various properties can be tracked continuously from the photons they emit. This has been used to measure the spatial first order coherence [10], the temporal first and second order correlation functions [11, 12] and even real time dynamics such as propagation [13].

The dynamical evolution and origin of the degree of coherence in a polariton condensate remain however unclear. Intriguing results have been recently reported of one order of magnitude increase of the ground state polaritons coherence time, by reducing particle fluctuations in the excited states [12]. Such experiments reveal the possibilities for the dynamical observation of condensation [14]. Also some theoretical studies have been reported based on stochastic simulations of the order parameter [15]. In this work, we pursue this goal both experimentally and theoretically, and track the dynamics of formation of a polariton BEC, following how the condensation forms and decays in a pulsed experiment.

Since polaritons have a spin degree of freedom that is passed to the polarization of the photon they emit, the buildup of off-diagonal elements in the density matrix (characteristic of coherent states) can be accessed

through the degree of linear polarization:

$$D_1 = 2 | \Re \langle a_{0\uparrow} a_{0\downarrow}^\dagger \rangle | / ( \langle a_{0\uparrow}^\dagger a_{0\uparrow} \rangle + \langle a_{0\downarrow}^\dagger a_{0\downarrow} \rangle ), \quad (1)$$

with  $a_{0\uparrow}$  and  $a_{0\downarrow}$  the field operators for spin-up (right-circular polarization) and spin-down (left-circular polarization) polaritons, respectively. If spin-up and spin-down polaritons are uncorrelated, with a thermal distribution and no determined phase relationship, the light is unpolarized. If, however, the two spin-projections are condensed with well defined order parameters  $\langle a_{0\uparrow} \rangle$ ,  $\langle a_{0\downarrow} \rangle$  that factorize the numerator of Eq. (1), the emitted light acquires a definite polarization. Therefore,  $D_1$  is linked to the degree of coherence of the condensate and to the imbalance of spin-up/spin-down polaritons [6, 11, 16, 17]. The spin degeneracy can be lifted producing a Zeeman splitting of polariton energies. If we can further assume that the two spin populations have similar evolutions, these can be modelled with a convolution of thermal and coherent states [16, 18] with time-dependent thermal and coherent fractions. In our case, we have observed experimentally that, except for a short transient after the pulsed excitation, spin-up and spin-down populations equalize and evolve similarly in time [19]. Therefore the degree of linear polarization is directly related to the degree of second order coherence (at zero delay)  $g^{(2)}$  of the polariton gas:  $D_1 \approx \sqrt{2 - g^{(2)}}$ . If the spin populations have very different dynamics, one has to keep track of the coherence degree of each of the two spin components and this simple expression no longer holds. Up to now, this relationship has been exploited for measuring the degree of coherence only in stationary situations [6, 11]. In this work, we use it to study experimentally the dynamics of condensation. Using simultaneous detection of energy- and time-resolved photoluminescence, together with the degree of linear polarization of the ground state, we monitor the formation and decay of the polariton condensed phase in the ground state after a circularly-polarized, pulsed excitation at high energy. Comparing our data with a phenomenological model, we investigate the evo-

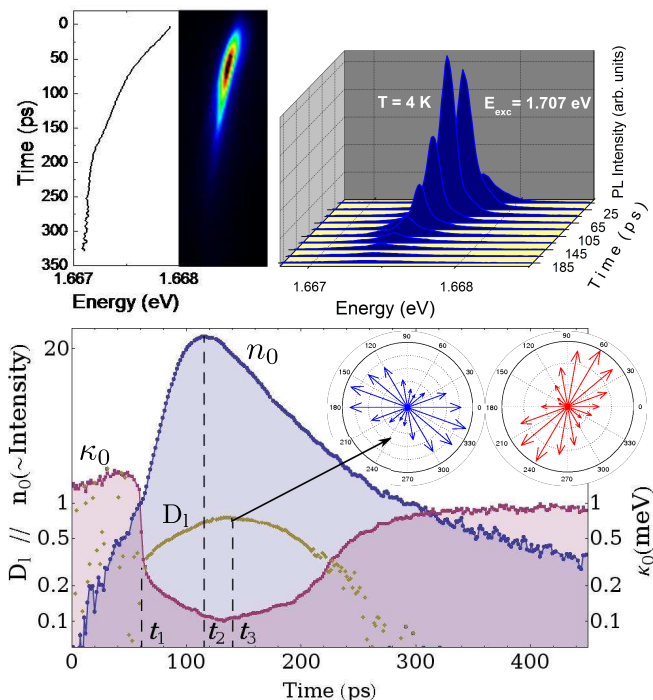


FIG. 1: (Color online) Experimental results on the dynamics of BEC formation after the arrival of the non-resonant pulse. (a) Emission energy from the ground state ( $k = 0$ ) as a function of time (left) and the corresponding photoluminescence intensity (right). The color code goes from black, no emission, to red, intense emission, saturating in a black central region. (b) Spectral lineshapes extracted from (a). (c) In blue dots, average condensate population  $n_0$  (normalized photoluminescence intensity); in purple squares, linewidth  $\kappa_0$  (meV) of the emission peak, limited by the spectral resolution of  $\sim 0.1$  meV; in brown rhombus, degree of linear polarization  $D_1$ . Times for coherence build-up ( $t_1$ ), maximum population ( $t_2$ ) and coherence ( $t_3$ ) are marked with dashed lines. Inset: polarization polar plot at  $t = t_3$  with maximum coherence for the present case (I) and for a second point in the sample (II).

lution of the condensate statistics and coherence.

In the experiments, polaritons are created in a CdTe-based microcavity grown by molecular beam epitaxy. The sample consists of a  $\text{Cd}_{0.4}\text{Mg}_{0.6}\text{Te}$   $2\lambda$ -cavity with top (bottom) distributed Bragg reflectors of 17.5 (23) pairs of alternating  $\lambda/4$ -thick layers of  $\text{Cd}_{0.4}\text{Mg}_{0.6}\text{Te}$  and  $\text{Cd}_{0.75}\text{Mn}_{0.25}\text{Te}$ . Four CdTe QWs of 50 Å thickness, separated by a 60 Å barrier of  $\text{Cd}_{0.4}\text{Mg}_{0.6}\text{Te}$ , are placed in each of the antinodes of the electromagnetic field. Exciton-photon coupling is achieved with a Rabi splitting of 23 meV; the sample is kept at 4 K and condensation is obtained around zero detuning between the exciton and the bare cavity dispersion. Photons are injected via circularly polarized, ps-long pulses tuned at the first minimum above the Bragg mirror stopband ( $\sim 40$  meV from the bottom of the dispersion) in order to guarantee the memory loss of the laser polarization and the coherence by the time polaritons are formed at the bottom

of the band. Light escaping from the microcavity is dispersed through a 0.5 m spectrometer and analyzed with a streak camera. This allows to resolve in time the intensity and energy of the emission of the ground state (Fig.1(a) and (b)), and simultaneously analyze the direction and linear degree of polarization of the emitted light together with the polariton linewidth (Fig.1(c) and insets). The direction of the linear polarization is pinned to a crystallographic axis, as has been observed with continuous pumping in a sample of the same batch growth [11] and with pulsed pumping in samples similar to ours [20]. Without this pinning, the polarization would average to zero, which is detrimental to our approach but is otherwise one of the most direct demonstration of symmetry breaking associated to the quantum phase transition, as reported by Baumberg *et al.* [6]. In our case, the direction of the pinning depends on the point of the sample, as shown in the insets (I) and (II) of Fig.1(c).

The non-resonant laser excitation creates a large population of carriers, at high energies, that form the polaritons. Thanks to the quick relaxation mechanisms, like phonon emission and polariton-polariton scattering [21], the population of polaritons relaxes into the fundamental state (with in-plane momentum  $k = 0$ ). Figure 1 depicts the experimental time evolution of the ground state after the arrival of the pulse at some time  $t < 0$ , till the complete decay of the condensate. The intensity of the light emitted by the condensate, first shown in Fig. 1(a)-right (in density plot), is normalized to represent the ground state population  $n_0$  in Fig. 1(c) (blue circles). The abrupt change into a nonlinear growth—associated with the onset of stimulated enhancement—is matched to 1. We note from the ground state energy (Fig. 1(a)), that the dispersion is already blueshifted (as compared to the long time energy, at  $t \geq 300$  ps), even when  $n_0$  is very small (at  $t \simeq 0$ ). This confirms that the blueshift is mainly due to exciton screening and carrier-carrier interaction in the exciton reservoir [22, 23, 24], and that it is only slightly affected by the ground state occupation. Note that the blueshift is always much smaller ( $< 1$  meV) than the Rabi splitting, so that the system remains in strong-coupling. As the reservoir depletes with time, the overall population and the blueshift monotonically decrease, while  $n_0$  first increases and then decreases. The coherence imprinted by the laser pulse and its original polarization is lost during this efficient cascade of decays, populating the ground state with initially uncorrelated polaritons. This is clear from the linear polarization  $D_1$  (brown rhombus in Fig. 1(c)), that takes some time to build up after  $n_0 \approx 1$ . Passed this particular time (corresponding to  $t_1 = 61$  ps in the figures) the system is above threshold with a condensed fraction and a phase locking of the spin-up and spin-down condensates. Stimulated scattering into the ground state becomes the dominating process and the population  $n_0$  grows up to a maximum (with  $\max(n_0) \approx 25$  at  $t_2 = 118$  ps). However, the co-

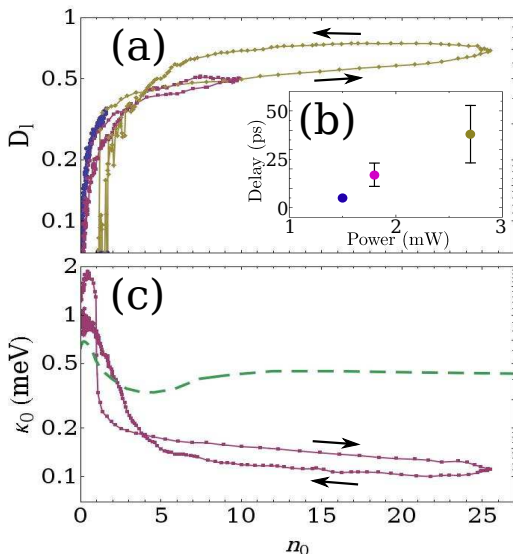


FIG. 2: (Color online) Hysteresis in  $D_1$  (a) and  $\kappa_0$  (c) as a function of  $n_0$ , with time running in the sense of the arrows. (a) Three experiments are shown with increasing excitation powers (the one under study in brown rhombus). (b) Growth with power of the delay between maximum population and coherence for these three cases. The linewidth of Ref. [3], under CW excitation, is given in (c) (dashed green) for comparison.

herence reaches its maximum,  $\max(D_1) = 0.75$ , at a later time,  $t_3 = 140$  ps, with a proper dynamics that does not follow instantaneously that of  $n_0$ :  $D_1$  decays for another 150 ps at a different rate than that of the population.  $D_1$  is represented as a function of  $n_0$  in Fig. 2(a), and compared with two other cases in order to make evident the existence of an hysteresis loop. As the excitation power is decreased, not only  $n_0$  and  $D_1$  decrease, but the hysteresis also gradually disappears.

The linewidth of the ground state emission is also dramatically affected by the condensation. In the simplest picture of a single mode with an effective pumping rate from all the other states  $W_0^{\text{out}} = \sum_k P_{k0}(1 + n_k)$  ( $n_k$  the population of the  $k$ th state) and a radiative decay rate  $\gamma_0$  at  $k = 0$ , the linewidth can be approximated by  $\kappa_0 = (W_0^{\text{out}} + \gamma_0)/(1 + n_0)$ . This expression is enough to understand qualitatively the linewidth dynamics. As shown in Fig. 1(c) (purple squares),  $\kappa_0$  drops dramatically at the phase transition due to the exponential growth of  $n_0$ . Close to the maximum population, the linewidth reaches the limiting value of our spectral resolution (0.1 meV). Note that  $\kappa_0$  not only depends on  $n_0$  but is also affected (broadened) by the populations of the levels feeding the ground state, which are enhanced before the transition takes place. The steady state value of  $\kappa_0 \rightarrow 0.9$  meV ( $t > 300$  ps) corresponds to the linewidth of the bare ground state polaritons,  $\gamma_0$ . This results in another hysteresis shown in Fig. 2(c). Although polaritons, being interacting bosons, also suffer screening due

to Coulomb interaction, this effect is only significant at extremely high polariton densities [25]. This regime is never reached in our experiment. Kasprzak *et al.* [3] observed under CW excitation an increase in the linewidth (dashed, green line in Fig. 2(c)) and attributed it to polariton-polariton interaction. However, we find that the ground state population is too small to produce this effect (the particle number should be three orders of magnitude higher). The reason for such a significant increase of the linewidth is more likely to be found in the high number of reservoir particles, much higher than  $n_0$  in the case of CW experiments. With our time dependent excitation, excluding the first few tenths of ps, the amount of particles in the reservoir is significantly smaller than that at the bottom of the polariton dispersion, reducing drastically this extra decoherence effect.

Our experiments on polariton coherence formation are supported by a simple two-level model (sketched in the inset of Fig. 3(a)), that links together the dynamics of the coherence degree with the population and the linear polarization. We work under the assumption—supported by the observation—that both spin components evolve similarly following this dynamics. We proceed in the spirit of the evaporative cooling description [26], that has been used before in models including polariton-polariton and photon-polariton scattering [25, 27]. A reservoir, state 1, is populated in an incoherent way from higher levels, what we describe with an effective time-dependent rate  $P_1(t)$  which has a Gaussian profile in time, reminiscent of the excitation of the laser at very high energy, with temporal effective width  $\Delta t_{\text{pulse}}$ . These particles are scattered incoherently into the ground state, level 0, at a different rate  $P_{10}$ . Both levels loose polaritons with decay rates  $\gamma_0$  and  $\gamma_1$ , respectively. We also include the inverse process of promoting polaritons up the branch at some small rate  $\gamma_{01}$ . This dynamics is described with Lindblad terms in a master equation of the ground-state/reservoir system. This leads to rate equations for the time dependent distributions of particles, which are solved numerically to compute the observables of interest ( $n_0$ ,  $g^{(2)}$ ,  $D_1$ , etc...). The linewidth is obtained from  $\kappa_0 \approx [\gamma_{01}(1 + n_1) + \gamma_0]/(1 + n_0)$ . In this model, the coherence builds up spontaneously, while other works [28] require a seed (such as an initial coherent state) in order to investigate the dynamics of coherence. The results, plotted in Fig. 3(a) with the same color code, are qualitatively similar to the experimental data in Fig. 1(c). With no need for more levels, we also reproduce the existence of a delay between maximum coherence and population. We find that when the effective pulse  $P_1(t)$  gets sharper in time (small  $1/\Delta t_{\text{pulse}}$ ), not only  $\max(n_0)$  and  $\max(D_1)$  are larger, but also the delay between them increases, as can be seen in Figs. 3(b) and (c). The delay can even become negative when the pulse is too flat. The origin and sign of the delay can be explained as follows: for a sharp and strong pulse, the



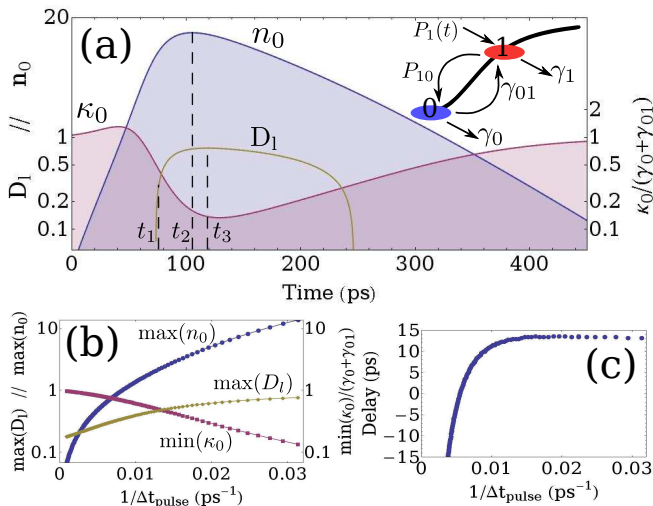


FIG. 3: (Color online) (a) Results from the theoretical model (sketched in inset):  $n_0$  (blue),  $D_1$  (brown) and  $\kappa_0$  (purple), as a function of time (rescaled to ps for comparison). In (b), the maximum  $\max(n_0)$ ,  $\max(D_1)$  and minimum  $\min(\kappa_0)$  values reached in the simulations as the effective pulse narrows (with increasing  $1/\Delta t_{\text{pulse}}$ ) down to the case in (a). The delay  $t_3 - t_2$  between  $\max(n_0)$  and  $\max(D_1)$  is also plotted in (c).

ground state population  $n_0$  rises so quickly that coherence formation cannot simultaneously build up (through stimulated interaction with the upper level), and settles to its own, intrinsic dynamics instead (the delay becomes independent of the pulse duration as this one gets narrower). With a flat pulse, on the other hand,  $n_0$  grows slowly and weakly, giving time to the condensate coherence to form together with it, possibly overtaking the dynamics for very long effective pulses and yielding a negative delay (Fig. 3(c)). Increasing the in-flow of particles (e.g., increasing  $P_{10}/\gamma_{01}$ ), also has a similar effect of enhancing the coherence and its rising time. On the other hand, the total intensity of the pulse is not determining the delay. This argument can be extended to the experiment, where a more intense pulse also results in a sharper profile for the effective excitation, given that the chain of de-excitations towards level 1 is more efficient, thanks to the density dependence of the exciton-exciton scattering [29].

Finally, although our simple model does not lead to a quantitative agreement with the experiments (time has been rescaled for a better comparison), it is of a fundamental character, since it contains the minimum number of elements to reproduce BEC formation and links together its essential features (population, coherence, linewidth and polarization). The model should include more levels in the de-excitation chain towards the ground state to reach to a quantitative agreement, not bringing, however, any essential new features into the description (as we have checked but which we do not discuss here).

In conclusion, we report the experimental observation

of the dynamics of a polariton condensate, created under a non-resonant, circularly polarized pulse, and the study of its coherence buildup and decay. We track the order parameter of the transition through the degree of linear polarization, that spontaneously builds up. This occurs when the average population of the ground state exceeds one and is accompanied by an abrupt decrease in the emission linewidth. The maximum degree of coherence that is achieved does not coincide in time with the maximum population, evidencing that the coherence of the condensate has its own particular dynamics. The pulsed excitation regime is a worthy tool revealing neatly the interplay of all the relevant quantities of polariton condensates and displaying the mechanisms of formation and decay of a BEC. We support our claims with a simple theoretical model.

We thank D. Porrás for fruitful discussions and the Spanish MEC (MAT2008-01555/NAN, QOIT-CSD2006-00019), CAM (S-0505/ESP-0200) and the IMDEA-Nanociencia for funding. EdV acknowledges the Newton Fellowship program and DS the Ramón y Cajal program.

- 
- [1] C. Weisbuch, M. Nishioka, A. Ishikawa, and Y. Arakawa, Phys. Rev. Lett. **69**, 3314 (1992).
  - [2] A. Kavokin, J. J. Baumberg, G. Malpuech, and F. P. Laussy, *Microcavities* (Oxford University Press, 2007).
  - [3] J. Kasprzak, M. Richard, S. Kundermann, A. Baas, P. Jeambrun, J. M. J. Keeling, F. M. Marchetti, M. H. Szymanska, R. André, J. L. Staehli, et al., Nature **443**, 409 (2006).
  - [4] R. Balili, V. Hartwell, D. Snoke, L. Pfeiffer, and K. West, Science **316**, 1007 (2007).
  - [5] S. Christopoulos, G. B. H. von Högersthal, A. J. D. Grundy, P. G. Lagoudakis, A. V. Kavokin, J. J. Baumberg, G. Christmann, R. Butté, E. Feltin, J.-F. Carlin, et al., Phys. Rev. Lett. **98**, 126405 (2007).
  - [6] J. J. Baumberg, A. V. Kavokin, S. Christopoulos, A. J. D. Grundy, R. Butté, G. Christmann, D. D. Solnyshkov, G. Malpuech, G. B. H. von Högersthal, E. Feltin, et al., Phys. Rev. Lett. **101**, 136409 (2008).
  - [7] D. Bajoni, P. Senellart, E. Wertz, I. Sagnes, A. Miard, A. Lemaître, and J. Bloch, Phys. Rev. Lett. **100**, 047401 (2008).
  - [8] M. Anderson, J. Ensher, M. Matthews, C. Wieman, and E. Cornell, Science **269**, 198 (1995).
  - [9] K. B. Davis, M.-O. Mewes, M. R. Andrews, N. J. van Druten, D. S. Durfee, D. M. Kurn, and W. Ketterle, Phys. Rev. Lett. **75**, 3969 (1995).
  - [10] H. Deng, G. S. Solomon, R. Hey, K. H. Ploog, and Y. Yamamoto, Phys. Rev. Lett. **99**, 126403 (2007).
  - [11] J. Kasprzak, M. Richard, A. Baas, B. Deveaud, R. André, J.-P. Poizat, and Le Si Dang, Phys. Rev. Lett. **100**, 067402 (2008).
  - [12] A. P. D. Love, D. N. Krizhanovskii, D. M. Whittaker, R. Boučekiouda, D. Sanvitto, S. A. Rizeiqi, R. Bradley, M. S. Skolnick, P. R. Eastham, R. André, et al., Phys. Rev. Lett. **101**, 067404 (2008).

- [13] A. Amo, D. Sanvitto, F. P. Laussy, D. Ballarini, E. del Valle, M. D. Martin, A. Lemaître, J. Bloch, D. N. Krizhanovskii, M. S. Skolnick, et al., *Nature* **457**, 291 (2009).
- [14] After the first submission of this text, more experiments on polariton BEC dynamics have been reported by G. Nardin *et al.*, arXiv:0905.2337.
- [15] D. Read, P. J. Membry, T. C. H. Liew, Y. G. Rubo, and A. V. Kavokin, arXiv:0807.0980 (2008).
- [16] F. P. Laussy, I. A. Shelykh, G. Malpuech, and A. Kavokin, *Phys. Rev. B* **73**, 035315 (2006).
- [17] I. A. Shelykh, Y. G. Rubo, G. Malpuech, D. D. Solnyshkov, and A. Kavokin, *Phys. Rev. Lett.* **97**, 066402 (2006).
- [18] G. Lachs, *Phys. Rev.* **138**, B1012 (1965).
- [19] M. D. Martin, G. Aichmayr, L. Viña, and R. André, *Phys. Rev. Lett.* **89**, 077402 (2002).
- [20] L. Kłopotowski, M. D. Martin, A. Amo, L. Viña, I. A. Shelykh, M. M. Glazov, G. Malpuech, A. V. Kavokin, and R. André, *Solid State Commun.* **139**, 511 (2006).
- [21] T. D. Doan, H. T. Cao, D. B. T. Thoai, and H. Haug, *Phys. Rev. B* **72**, 085301 (2005).
- [22] N. Peyghambarian, H. M. Gibbs, J. L. Jewell, A. Antonetti, A. Migus, D. Hulin, and A. Mysyrowicz, *Phys. Rev. Lett.* **53**, 2433 (1984).
- [23] S. Schmitt-Rink, C. Ell, and H. Haug, *Phys. Rev. B* **33**, 1183 (1986).
- [24] C. Ciuti, P. Schwendimann, B. Deveaud, and A. Quattropani, *Phys. Rev. B* **62**, R4825 (2000).
- [25] D. Porras and C. Tejedor, *Phys. Rev. B* **67**, 161310(R) (2003).
- [26] M. Holland, K. Burnett, C. Gardiner, J. I. Cirac, and P. Zoller, *Phys. Rev. A* **54**, R1757 (1996).
- [27] F. P. Laussy, G. Malpuech, A. Kavokin, and P. Bigenwald, *Phys. Rev. Lett.* **93**, 016402 (2004).
- [28] Y. G. Rubo, F. P. Laussy, G. Malpuech, A. Kavokin, and P. Bigenwald, *Phys. Rev. Lett.* **91**, 156403 (2003).
- [29] L. Muñoz, E. Pérez, L. Viña, and K. Ploog, *Phys. Rev. B* **51**, 4247 (1995).